KSABC
The Korean Society for Applied Biological Chemistry

Anticancer activities of cyclohexenone derivatives

Soon Young Shin[1], Jihyun Park[2], Yearam Jung[2], Young Han Lee[1], Dongsoo Koh[3], Youngdae Yoon[4*] and Yoongho Lim[2*]

Abstract

We designed 21 ethyl 3,5-diphenyl-2-cyclohexenone-6-carboxylate derivatives to identify compounds exhibiting anticancer activity. To measure the inhibitory effects of the compounds on cancer cell growth, a long-term survival clonogenic assay was performed. Since compounds containing a cyclohexenone moiety inhibit the enzyme acetyl-cholinesterase, an in vitro acetylcholinesterase assay was performed for all 21 cyclohexenone derivatives. To examine the effect of the derivative that exhibited the best cancer cell growth inhibition on the induction of apoptosis by demonstrating the activation of caspases and apoptosis regulatory proteins, immunoblotting and immunofluorescence microscopic analyses were performed. The binding mode between the cyclohexenone derivatives and acetylcholinesterase was elucidated at the molecular level using in silico docking. Druggability was evaluated based on ligand efficiency.

Keywords: Acetylcholinesterase, Anticancer, Apoptosis, Cyclohexenone derivatives, Caspase

Introduction

The aim of the study was to evaluate the anticancer activities of ethyl 3,5-diphenyl-2-cyclohexenone-6-carboxylate derivatives in HCT116 human colon cancer cells. Chalcone contains two phenyl rings connected by an α,β-unsaturated carbonyl group. More than a thousand chalcones were reported in PubChem (https://pubchem.ncbi.nlm.nih.gov/) and several tens of thousands could be searched in SciFinder (https://scifinder.cas.org/). The increased research interest in chalcones stems from its diverse biological activities, including anti-inflammatory, antioxidant, antifungal, antimicrobial, and antimalarial, among others [1–6]. Mdl 27,048 (2′,5′-dimethoxy-4-(dimethylamino)chalcone) inhibited tubulin polymerization [7]. Butein (3,4,2′,4′-tetrahydroxychalcone) inhibited inhibitor of nuclear factor kappa-B
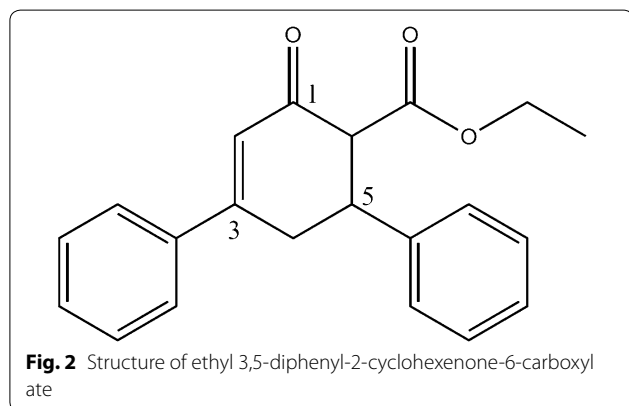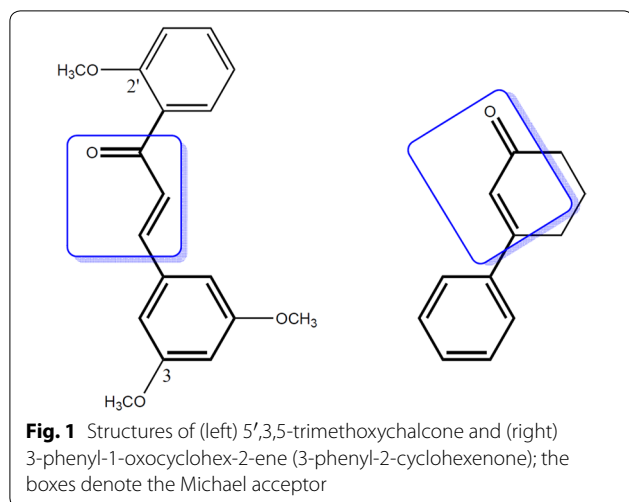
kinase subunit beta (IKKβ), which resulted in the translocation of the nuclear factor kappa-light-chain enhancer of activated B cells [7]. Xanthohumol (4,2′,4′-trihydroxy-6′-methoxy-3′-(methylbut-2-enyl)chalcone) inhibited aromatase, the inhibitors of which were used for the treatment of breast cancer [8]. Xanthoangelol (2′,4′,4-trihydroxy-3′-((2E)-3,7-dimethylocta-2,6-dienyl)chalcone) inhibited aurora A and B kinases, which were known oncoproteins [9]. In our previous studies, 2-hydroxy-4-methoxy-2′,3′-benzochalcone was found to inhibit tubulin polymerization [10] and 2′-hydroxy-2,4,6-trimethoxy-5′,6′-naphthochalcone induced G2/M cell cycle arrest and apoptosis [11]. An anticancer effect was common among these chalcones. The α,β-unsaturated carbonyl group in chalcones acted as a Michael acceptor, which can form a covalent bond with the thiol group in cysteine or glutathione. The formation of the covalent bond limited the elevation of the glutathione level. In our previous research, we demonstrated that 5′,3,5-trimethoxychalcone killed cancer cells selectively via the generation of reactive oxygen species (ROS) [12]. In cancer cells, increased levels of ROS led to cell death; however,

*Correspondence: shim0924@konkuk.ac.kr; yoongho@konkuk.ac.kr
[2] Division of Bioscience and Biotechnology, Konkuk University, Seoul 05029, Korea
[4] Department of Environmental Health Science, Konkuk University, Seoul 05029, Korea
Full list of author information is available at the end of the article

Springer Open

Shin *et al. Appl Biol Chem*   (2020) 63:82

Page 2 of 9

Fig. 1 Structures of (left) 5′,3,5-trimethoxychalcone and (right) 3-phenyl-1-oxocyclohex-2-ene (3-phenyl-2-cyclohexenone); the boxes denote the Michael acceptor

Fig. 2 Structure of ethyl 3,5-diphenyl-2-cyclohexenone-6-carboxylate

in normal cells, these species stimulated cellular proliferation [13, 14]. Besides, the Michael acceptor in chalcones activated Kelch-like ECH-associated protein 1 [15]. Therefore, the authors of that study attempted to modify the chalcone, retaining the Michael acceptor. A study reported that 3,5-diaryl-2-cyclohexenone attenuated heart failure in a zebra fish model [16]. Figure 1 (left and right) presents the structures of 5′,3,5-trimethoxychalcone and 3-phenyl-1-oxocyclohex-2-ene (3-phenyl-2-cyclohexenone), respectively. The boxes in the structures indicate the Michael acceptor calyxol (ethyl 3-methyl-5-pentyl-2-cyclohexenone-4-carboxylate), which has been reported to have bed bug repellency [17]. As mentioned above, because compounds containing cyclohexenone or/and carboxylate moiety showed various biological activities, we designed derivatives of ethyl 3,5-diphenyl-2-cyclohexenone-6-carboxylate (Fig. 2).

Of the multiple methods that can be used to screen anticancer compounds, we opted for a clonogenic long-term survival assay, given its ability to distinguish small differences in the antitumor activity caused by

compounds with similar structures [18]. To verify the biological activity of the cyclohexenone derivatives, we determined the activation of the apoptosis regulatory protein caspases [19], through immunoblotting and immunofluorescence microscopy in HCT116 colon cancer cells. Compounds containing a cyclohexenone moiety have been reported to inhibit acetylcholinesterase (AChE) [20]. In this study, we predicted that ethyl 3,5-diphenyl-2-cyclohexenone-6-carboxylate derivative binds to AChE using an in silico docking experiments. The druggability of the cyclohexenone derivatives was evaluated based on ligand efficiency. Our results suggest that ethyl 3,5-diphenyl-2-cyclohexenone-6-carboxylate derivatives inhibit AChE activity and trigger apoptosis in HCT116 colon cancer cells.

Materials and methods

Twenty-one derivatives of ethyl 3,5-diphenyl-2-cyclohexenone-6-carboxylate (listed in Table 1) were prepared according to the previous report [21]. A clonogenic long-term survival assay was performed in HCT116 human colon cancer cells, as previously described [22]. HCT116 cells were obtained from the American Type Culture Collection (ATCC, Rockville, MD, USA) and maintained in Dulbecco's modified Eagle's medium supplemented with 10% (v/v) heat-inactivated fetal bovine serum (HyClone, Logan, UT, USA). The cells were seeded into 24-well tissue culture plates (Becton Dickinson Immunocytometry Systems, San Jose, CA, USA) at 3×10^3 cells per well. After attachment, the cells were exposed to different concentrations of the derivatives (0, 5, 10, 20, and 40 μM) for 7 days, followed by fixation in 6% (w/v) glutaraldehyde and staining with 0.1% (w/v) crystal violet [23]. For all of these analyses, previously reported methods were followed [25].

Immunoblotting was performed as described previously with minor modifications [24]. Briefly, HCT116 cells were lysed in a buffer containing 20 mM 4-(2-hydroxyethyl)-1-piperazineethanesulfonic acid (HEPES; pH 7.2), 1% Triton X-100, 10% glycerol, 150 mM sodium chloride (NaCl), 10 μg/ml leupeptin, and 1 mM phenylmethylsulfonyl fluoride (PMSF). Whole-cell lysates were electrophoresed on a 10% sodium dodecyl sulfate (SDS)-polyacrylamide gel and transferred onto nitrocellulose membranes (Bio-Ras, Richmond, CA, USA). After blocking the membranes with 10% skim milk in Tris saline buffer (10 mM Tris–HCl, pH 8.0, 150 mM NaCl, and 0.1% Tween 20) for 1 h at 25 ℃, primary antibodies were added and the membranes were incubated overnight at 4 ℃. Primary antibodies against cleaved caspase-9, cleaved caspase-7 (Asp198), cleaved caspase-3 (Asp198), and poly(ADP-ribose) polymerase (PARP) were obtained from Cell Signaling Technology (Beverly,

Shin *et al. Appl Biol Chem*   (2020) 63:82

Page 3 of 9

Table 1 List of cyclohexenone derivatives

Derivative	Name	IC$_{50}$/μM	logP	MW
1	ethyl 3-(2-hydroxyphenyl)-5-(naphthalen-1-yl)-2-cyclohexenone-6-carboxylate	89.39	4.48	386.44
2	ethyl 3-(2-hydroxy-6-methoxyphenyl)-5-(naphthalen-1-yl)-2-cyclohexenone-6-carboxylate	127.35	4.35	416.47
3	ethyl 3-(2-hydrox-4,5-dimehoxyyphenyl)-5-(naphthalen-1-yl)-2-cyclohexenone-6-carboxylate	7.83	4.22	446.49
4	ethyl 3-(2-hydroxy-4,6-dimethoxyphenyl)-5-(naphthalen-1-yl)-2-cyclohexenone-6-carboxylate	Note determined	4.22	446.49
5	ethyl 3-(2-hydroxy-4-methoxyphenyl)-5-(naphthalen-1-yl)-2-cyclohexenone-6-carboxylate	110.81	4.35	416.47
6	ethyl 3-(2-hydroxyphenyl)-5-(naphthalen-2-yl)-2-cyclohexenone-6-carboxylate	90.00	4.48	386.44
7	ethyl 3-(2-hydroxy-6-methoxyphenyl)-5-(naphthalen-2-yl)-2-cyclohexenone-6-carboxylate	98.37	4.35	416.47
8	ethyl 3-(2-hydroxy-4,5-dimethoxyphenyl)-5-(naphthalen-2-yl)-2-cyclohexenone-6-carboxylate	1.03	4.22	446.49
9	ethyl 3-(2-hydroxy-4-methoxyphenyl)-5-(naphthalen-2-yl)-2-cyclohexenone-6-carboxylate	122.81	4.35	416.47
10	ethyl 3-(2-hydroxyphenyl)-5-(2-methoxynaphthalen-1-yl)-2-cyclohexenone-6-carboxylate	108.18	4.35	416.47
11	ethyl 3-(2-hydroxy-5-methoxyphenyl)-5-(2-methoxynaphthalen-1-yl)-2-cyclohexenone-6-carboxylate	5.34	4.22	446.49
12	ethyl 3-(2-hydroxy-6-methoxyphenyl)-5-(2-methoxynaphthalen-1-yl)-2-cyclohexenone-6-carboxylate	80.07	4.22	446.49
13	ethyl 3-(2-hydroxy-4,5-methoxyphenyl)-5-(2-methoxynaphthalen-1-yl)-2-cyclohexenone-6-carboxylate	1.74	4.10	476.52
14	ethyl 3-(2-hydroxy-4,6-dimethoxyphenyl)-5-(2-methoxynaphthalen-1-yl)-2-cyclohexenone-6-carboxylate	133.12	4.10	476.52
15	ethyl 3-(2-hydroxyphenyl)-5-(naphthalen-1-yl)-2-cyclohexenone-6-carboxylate	72.87	4.35	416.47
16	ethyl 3-(2-hydroxyphenyl)-5-(4-methoxynaphthalen-1-yl)-2-cyclohexenone-6-carboxylate	2.27	4.22	446.49
17	ethyl 3-(2-hydroxy-6-methoxyphenyl)-5-(4-methoxynaphthalen-1-yl)-2-cyclohexenone-6-carboxylate	115.37	4.22	446.49
18	ethyl 3-(2-hydroxy-4,6-dimethoxyphenyl)-5-(4-methoxynaphthalen-1-yl)-2-cyclohexenone-6-carboxylate	115.09	4.10	476.52
19	ethyl 3-(2-hydroxy-6-methoxyphenyl)-5-(2,3-dimethoxynaphthalen-1-yl)-2-cyclohexenone-6-carboxylate	85.88	4.10	476.52
20	ethyl 3-(1-hydroxynaphthalen-2-yl)-5-(2-methoxyphenyl)- 2-cyclohexenone-6-carboxylate	72.18	4.35	416.47
21	ethyl 3-(2-hydroxy-4-methoxyphenyl)-5-(2-methoxynaphthalen-1-yl)-2-cyclohexenone-6-carboxylate	0.93	4.22	446.49

IC$_{50}$, half-maximal inhibitory concentrations values by in vitro acetylcholinesterase enzyme assay; logP, the logarithm of partition coefficient values calculated using the Sybyl/MOLCAD module; MW, molecular weight

MA, USA), and antibodies against glyceraldehyde-3-phosphate dehydrogenase (GAPDH) were purchased from Santa Cruz Biotechnology (Santa Cruz, CA, USA). After washing the membranes thrice with Tris saline buffer, horseradish peroxidase (HRP)-conjugated secondary antibodies (Cell Signaling Technology) were added and incubated for 4 h at 25 ℃. After washing the membranes five times with TBST, the blots were developed using an Amersham ECL Western Blotting Detection Kit (GE Healthcare Life Science, Chicago, IL, USA).

An in vitro acetylcholinesterase enzyme activity assay was performed using an acetylcholinesterase assay kit (fluorometric-green; ab138872; Abcam, Cambridge, UK). Thiocholine produced from the hydrolysis of acetylthiocholine by AChE can be quantified using thiol green indicator. The intensity of thiol green indicator was measured on an FS-2 fluorescence spectrophotometer (Scinco, Seoul, Korea) fitted with a xenon lamp and bandwidth-adjustable filters for the excitation and emission wavelengths. Samples of all 21 derivatives were dissolved in dimethylsulfoxide and adjusted to 1, 5, 10, 50, and 80 μM concentrations. Donepezil (used as a reference drug) solutions were prepared at 0.001,

0.01, 0.1, 1, 5, and 10 μM concentrations. The excitation and emission wavelengths were 490 and 520 nm, respectively. IC$_{50}$ values were determined using Sigma-Plot, following the manufacturer's protocol.

Immunofluorescence staining was conducted as described previously [26]. HCT116 cells were cultured on coverslips and treated with derivative **21** for 12 h. After fixing the cells with 4% paraformaldehyde and permeabilizing them with 0.1% (v/v) Triton X-100, the cells were incubated with primary antibodies against α/β-tubulin and cleaved caspase-7 for 2 h at 25 ℃. It was probed with Alexa Fluor 488- (for α/β-tubulin; green signal) and Alexa Fluor 555-conjugated (for cleaved caspase-7; red signal) secondary antibodies for 30 min at 25 ℃. Nuclear DNA was counterstained with 1 μg/mL Hoechst 33,258 for 10 min (blue signal). Fluorescence was examined under an EVOS FL fluorescence microscope (Advanced Microscopy Group; Bothell, WA, USA).

As a three-dimensional (3D) structure of AChE, 4ey7.pdb deposited in the protein data bank (PDB) was selected [27] for the in silico docking experiments conducted on a Linux PC using the Sybyl program (Tripos,

Shin *et al. Appl Biol Chem*   (2020) 63:82

Page 4 of 9

St. Louis, MO, USA). The experimental procedures followed have been described previously in detail [28].

Results and discussion

The 21 cyclohexenone derivatives used in this study contained 3 substituents, including 3,5-diphenyl rings and ethyl 6-carboxylate (Fig. 2). The 3,5-diphenyl group was substituted with 1-naphthalene or 2-naphthalene. The clonogenic assay shows that most of the derivatives inhibited the clonogenic ability of HCT116 cells at concentrations of 20–40 μM (Fig. 3). The 1-naphthalenyl substituents exhibited better inhibitory activity on the clonogenicity of HCT116 cells than the 2-naphthalenyl substituents, and the number and position of the substituents attached to the 3-phenyl ring, including the hydroxy and methoxy groups, did not affect the clonogenicity of HCT116 cells (Table 1). These data suggest that cyclohexenone derivatives used in this study exhibit anticancer properties (Fig. 4).

AChE is a serine hydrolase found at cholinergic synapses and neuromuscular junctions. It plays a crucial role in terminating neuronal transmission by hydrolyzing acetylcholine into acetic acid and choline [30]. In addition to the classical function of acetylcholine hydrolysis, AChE also exerts non-cholinergic functions such as the promotion of apoptosis in HeLa cells [31] and fibroblasts [32]. However, several studies reported that acetylcholine induces the proliferation of gastric cancer cells [33] and stimulates lung cancer growth [34, 35]. The enzymatic activity of AChE is enhanced in meningiomas, gliomas, and vestibular nerve schwannomas [36–39]. Thus, AChE functions differently in different tissue types. In human colon cancer cells, the stimulation of the muscarinic cholinergic M3 receptor induced cellular proliferation [40] and stimulated migration and invasion [41, 42]. In addition, acetylcholine is synthesized and mediates the autocrine stimulation of colon cancer cell proliferation [43]. These findings suggest that AChE inhibitors may be useful chemotherapeutic agents against colon cancer.

As compounds containing a cyclohexenone moiety can inhibit AChE [44], we tested whether cyclohexenone derivatives inhibit AChE enzyme activity. In vitro AChE enzyme activity assay shows that the half-maximal enzyme inhibitory concentration (IC_{50}) values ranged from 0.93 to 133.12 μM (Fig. 5 and Table 1). Among them, derivative **21** exhibited the best AChE inhibitory activity (IC_{50} = 0.93 μM). The IC_{50} value of donepezil, 2-((1-benzylpiperidin-4-yl)methyl)-5,6-dimethoxy-2,3-dihydro-1*h*-inden-1-one, known as an AChE inhibitor, was determined to be 0.13 μM under the same experimental conditions. The trade name of donepezil is Aricept, which is used in the treatment of Alzheimer's disease [45].

Caspases are cysteine-dependent proteases that mediate the apoptosis triggered by various anticancer agents [19]. Caspases are activated via proteolytic cleavage during the initiation (caspase-9) and execution stages (caspase-3 and -7) of apoptosis [19]. To investigate whether the inhibition of AChE induces apoptosis, we treated HCT116 cells with 50 μM derivative **21**, which showed the highest AChE inhibitory activity, and examined the activation of caspases through immunoblotting. Upon
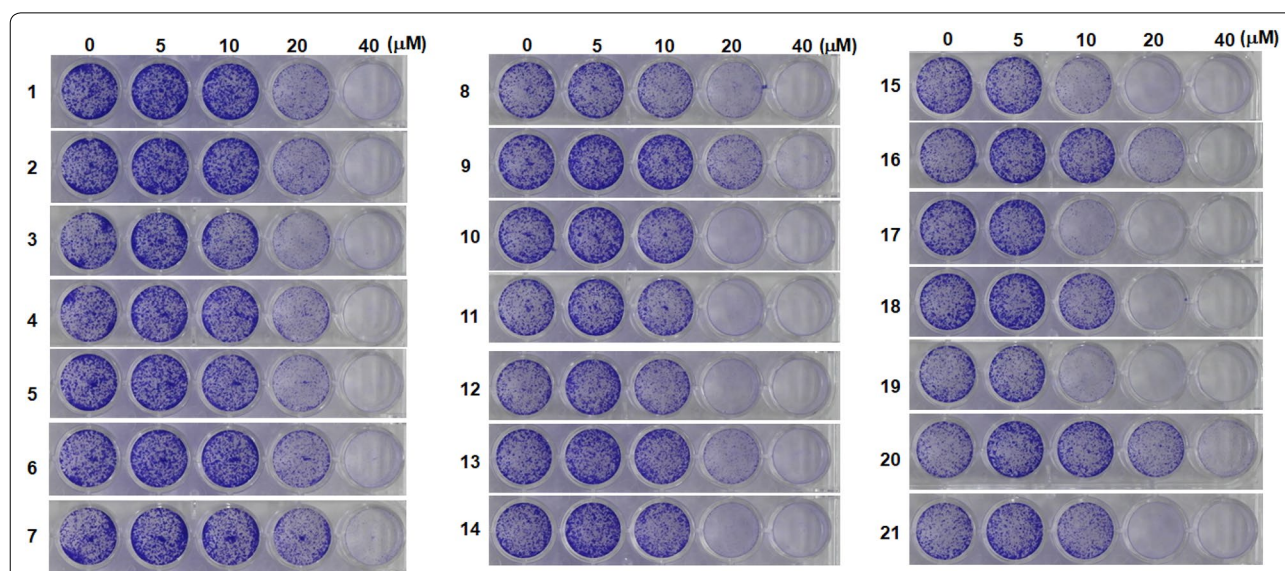

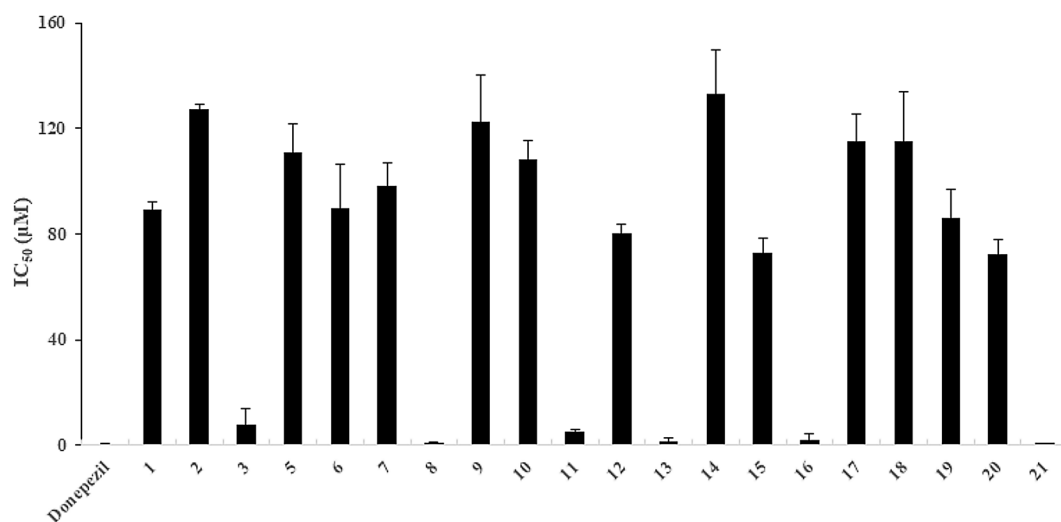**Fig. 3** Effect of 21 cyclohexenone derivatives on the clonogenicity of HCT116 cells

Shin *et al. Appl Biol Chem* (2020) 63:82

Page 5 of 9

Fig. 4 Effect of 21 cyclohexenone derivatives on AChE activity in vitro. Bars represent mean ± standard deviation ($n = 3$). IC_{50}, half-maximal enzyme inhibitory concentration; Donepezil, an AChE inhibitor reference compound.

treatment with derivative **21**, the proteolytic fragments of the initiator caspase (caspase-9) and executioner caspases (caspase-3 and -7) increased in a time-dependent manner (Fig. 5a). Poly(ADP-ribose) polymerase (PARP) is a substrate protein of caspase-3 and -7 [29]. The extent of the proteolytic cleavage of PARP was also increased as a function of time, following treatment with derivative **21** (Fig. 5a). Immunofluorescence microscopy also showed high levels of cleaved caspase-7 upon treatment with derivative **20** (Fig. 5b). Notably, fragmented nuclei, a characteristic of apoptotic cells, appeared after treatment with derivative **21**. These data suggest that derivative **21** triggers apoptosis via the activation of the caspase cascade in HCT116 colon cancer cells.

To elucidate the binding mode of AChE and cyclohexenone derivatives, we conducted in silico docking experiments using derivative **21**. Multiple 3D structures of AChE are available in the PDB. Even the PDB structures 1f8u.pdb and 4bdt.pdb contained the highest number of residues, with resolutions of 2.90 Å and 3.10 Å, respectively [46, 47]; they did not contain donepezil as the ligand, which was used as a reference compound in the current in vitro AChE enzyme assay. Therefore, 4ey7.pdb containing donepezil as its ligand and with a resolution of 2.35 Å was selected for in silico docking [27]. Although human AChE consists of 614 amino acids, 4ey7.pdb contains 542 amino acid residues (Gly33–Thr574), with homodimer polypeptides A and B. Since chain A contained more unmodeled residues than chain B, the latter was chosen for docking purposes. The apo-protein of chain B, prepared using the Sybyl program, was subjected to energy

minimization. The root mean square deviation between the crystallographic structure and energy minimized apo-protein was 0.22 Å. Residues in the binding site were determined via LigPlot analysis [48]: Try103, Trp117, Gly152, Tyr155, Glu233, Ser234, Trp317, Ser324, Phe326, Tyr368, Phe369, Tyr372, and His478. The 3D structure of derivative **21** was determined based on the 3D structure of 5-pentafluorophenyl-3-phenyl-2-cyclohexenone available at PubChem. The Sybyl program provides a flexible docking method. To confirm the accuracy of the docking procedures, the donepezil ligand of 4ey7.pdb that was docked onto the apo-protein of AChE chain B was observed to dock well (Additional file 1: Fig. S1). The Sybyl program generated 30 ligand–protein complexes owing to the 30 repeated iterations. The binding energy obtained from the docking results ranged between 13.55 and − 10.62 kcal/mol. Likewise, in silico docking for derivative **21** revealed the binding energy to range from − 11.96 to − 10.91 kcal/mol. The derivative **21** ligands generated by 30 iteraton were docked into the apo-AChE protein well (Additional file 1: Fig. S2). The complex with the lowest binding energy showed the best docking pose (Additional file 1: Fig. S3) and was thus subjected to analysis using LigPlot (Additional file 1: Fig. S4). Nine residues, including Trp286, Leu289, Glu292, Val294, Arg296, Phe297, Phe338, Tyr341, and Gly342, showed hydrophobic interactions, and two residues, Ser293 and Phe295, formed hydrogen bonds (H-bonds). H-bonds were observed between the amino proton of the peptide bond of Ser293 and the ketone oxygen of carboxylic acid (3.11 Å) and between the amino proton
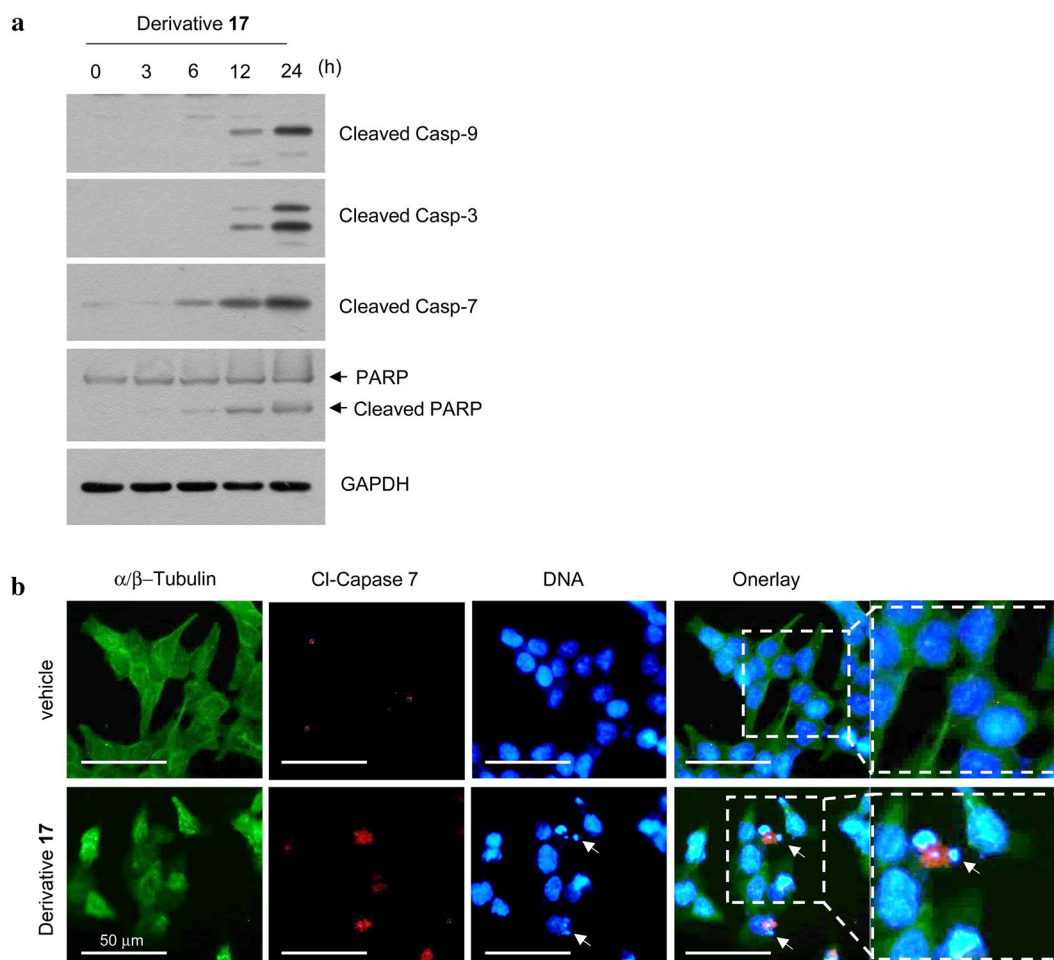
Shin *et al. Appl Biol Chem*   (2020) 63:82

Page 6 of 9

Fig. 5 Effect of derivative **21** on the activation of the caspase cascade. **a** HCT116 cells were treated with 50 μM derivative **21** for various durations of time (0–24 h), and whole-cell lysates were subjected to immunoblotting using antibodies specific for the cleaved caspases. Glyceraldehyde-3-phosphate dehydrogenase (GAPDH) was used as an internal control to ensure the same amount of protein loading. **b** HCT116 cells cultured on coverslips were treated with 50 μM derivative **21** for 12 h. The cells were fixed and incubated with antibodies against α/β-tubulin and cleaved caspase-7 for 2 h, followed by incubation with AlexaFluor 488- (green signal) and AlexaFluor 555-conjugated (red signal) secondary antibodies for 30 min. Nuclear DNA was stained with 0.1 μg/mL Hoechst 33,258 for 10 min (blue signal). Arrows indicate the apoptotic nuclear fragments. Fluorescence-positive cells were examined under an EVOS FL® fluorescence microscope. Dotted boxes are enlarged on the right. Size bars, 50 μm

of the peptide bond of Phe295 and the oxygen of the methoxy group attached to the phenyl ring (2.89 Å). The 3D image of the binding site of the derivative **21**–AChE complex was generated using PyMol program (The PyMOL Molecular Graphics System, Version 2.0 Schrödinger, LLC. Portland, OR, USA) (Fig. 6). The reason for the low binding energy of the derivative **21**–AChE complex compared to the donepezil–AChE complex may be related to their IC_{50} values, i.e., 0.93 μM and 0.13 μM, respectively. Besides, while donepezil was docked inside the binding site (Additional file 1: Fig. S1), derivative **21** was docked at the entrance of the binding site (Additional file 1: Fig. S3).

The molecular weights of the 21 cyclohexenone derivatives ranged between 386 and 476 Da (Table 1). While 18 derivative compounds were novel, derivatives **1**, **10**, and **20**, though not published, were registered with the Chemical Abstract Service (https://www.cas.org/), vide registration numbers, 1632161-14-8, 1194722-11-6, and 52220-43-6, respectively. Lead optimization, necessary to obtain novel and active compounds, resulted in increased molecular weights, with a subsequent enhancement in hydrophobicity as well [49]. Hydrophobicity can be predicted by the logP values. In this study, the logP values that were calculated using the Sybyl/MOLCAD module, ranged from 4.10 to 4.48 (Table 1). Because highly
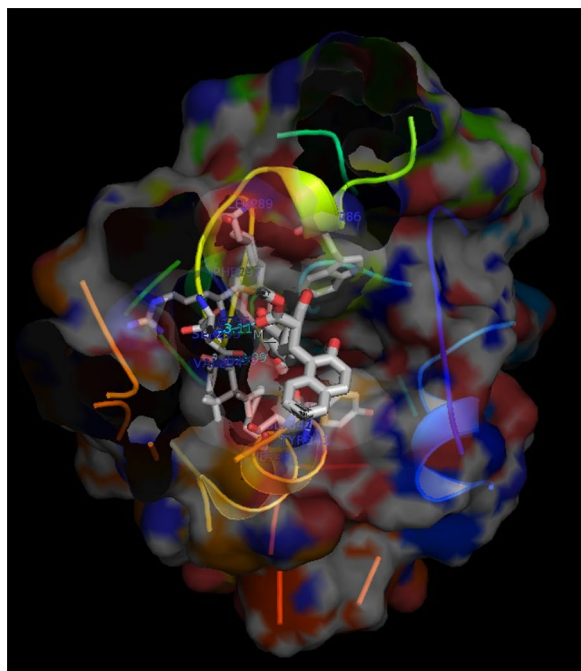
Shin *et al. Appl Biol Chem*   (2020) 63:82

Page 7 of 9

Fig. 6 Three-dimensional (3D) image of the binding site of the derivative **21**-acetylcholinesterase complex generated by PyMol (The PyMOL Molecular Graphics System, Version 2.0 Schrödinger, LLC. Portland, OR, USA)

lipophilic compounds have low solubility, in vivo experiments, including the preclinical phase, are challenging to perform. Therefore, this requires an additional delivery system.

Ligand efficiency (LE) is the ratio of the ligand affinity for the target molecules to the number of heavy atoms except for hydrogen atoms [49], which has been used to rank hit compounds for drug development. LE can be obtained from the equation as follows:

$$LE = -\Delta G/HA$$

where ΔG and HA denote the Gibbs free energy change associated with the binding of the ligand–protein complex and the number of non-hydrogen atoms, respectively [50]. The LE value for the derivative **21**–apo-AChE complex obtained using this equation was 0.36 ($\Delta G = -11.88$ kcal/mol, HA = 33), which falls into the criteria of LE values for drug-like compounds [50]. Therefore, the cyclohexenone derivatives obtained in this research can be considered potent chemotherapeutic agents. However, the study has some limitations. The limited number of tested derivatives in this study may not provide sufficient evidence for the chemotherapeutic potential. Further in vivo studies are needed to confirm the correlation between the cyclohexenone

derivative-induced AChE inhibitory activity and anticancer property.

Supplementary information

Supplementary information accompanies this paper at https://doi.org/10.1186/s13765-020-00567-1.

Additional file 1: Fig. S1. Image of donepezil—apo-protein of acetylcholinesterase chain B complex obtained from the current docking process. The circle denotes donepezil. **Fig. S2.** Image of derivative **21** docked into acetylcholinesterase. **Fig. S3.** Image of the derivative **21**—apo-protein of acetylcholinesterase chain B complex. The circle denotes derivative **21**. **Fig. S4.** Binding site of the derivative **21**—apo-acetylcholinesterase complex analyzed using LigPlot.

Abbreviations
IKKβ: Inhibitor of nuclear factor kappa-B kinase subunit beta; ROS: Reactive oxygen species; AChE: Acetylcholinesterase; PDB: Protein data bank; IC_{50}: Half maximal enzyme inhibitory concentration 50; LE: Ligand efficiency; HEPES: 4-(2-Hydroxyethyl)-1-piperazineethanesulfonic acid; PMSF: Phenylmethylsulfonyl fluoride; SDS: Sodium dodecyl sulfate; HRP: Horse radish peroxidase; GAPDH: Glyceraldehyde-3-phosphate dehydrogenase.

Authors' contributions
YY and YL participated in the study design. SYS and YHL carried out molecular and cellular experiments. JP and YJ performed the AChE enzyme activity assay. DK carried out chemical synthesis. SYS and YL wrote the manuscript. All authors read and approved the final manuscript.

Availability of data and materials
The datasets used and analyzed in this study are available from the corresponding author on reasonable request.

Competing interests
The authors declare that there is no conflict of interest.

Author details
[1] Department of Biological Sciences, Konkuk University, Seoul 05029, Korea. [2] Division of Bioscience and Biotechnology, Konkuk University, Seoul 05029, Korea. [3] Department of Applied Chemistry, Dongduk Women's University, Seoul 02748, Korea. [4] Department of Environmental Health Science, Konkuk University, Seoul 05029, Korea.

References
1. Singh P, Anand A, Kumar V (2014) Recent developments in biological activities of chalcones: a mini review. Eur J Med Chem 85:758–777
2. Mahapatra DK, Bharti SK, Asati V (2017) Chalcone derivatives: anti-inflammatory potential and molecular targets perspectives. Curr Top Med Chem 17(28):3146–3169
3. Lin Y, Zhang M, Lu Q, Xie J, Wu J, Chen C (2019) A novel chalcone derivative exerts anti-inflammatory and anti-oxidant effects after acute lung injury. Aging 11(18):7805–7816
4. Zheng Y, Wang X, Gao S, Ma M, Ren G, Liu H, Chen X (2015) Synthesis and antifungal activity of chalcone derivatives. Nat Prod Res 29(19):1804–1810

Shin *et al. Appl Biol Chem*   (2020) 63:82

Page 8 of 9

5. Inamullah F, Fatima I, Khan S, Kazmi MH, Malik A, Tareen RB, Abbas T (2017) New antimicrobial flavonoids and chalcone from Coluteaarmata. Arch Pharm Res 40(8):915–920

6. Kumar D, Kumar M, Kumar A, Singh SK (2013) Chalcone and curcumin derivatives: a way ahead for malarial treatment. Mini Rev Med Chem 13(14):2116–2133

7. Peyrot V, Leynadier D, Sarrazin M, Briand C, Rodriquez A, Nieto JM, Andreu JM (1989) Interaction of tubulin and cellular microtubules with the new antitumor drug MDL 27048. A powerful and reversible microtubule inhibitor. J Biol Chem 264:21296–21301

8. Lee D, Bhat KP, Fong HH, Farnsworth NR, Pezzuto JM, Kinghorn AD (2001) Aromatase inhibitors from Broussonetiapapyrifera. J Nat Prod 64:1286–1293

9. Limper C, Wang Y, Ruhl S, Wang Z, Lou Y, Totzke F, Kubbutat MHG, Chovolou Y, Proksch P, Wätjen W (2013) Compounds isolated from Psoralea corylifolia seeds inhibit protein kinase activity and induce apoptotic cell death in mammalian cells. J Pharm Pharmacol 65:1393–1408

10. Shin SY, Kim J, Yoon H, Choi Y, Koh D, Lim Y, Lee YH (2013) Novel antimitotic activity of 2-hydroxy-4-methoxy-2′,3′-benzochalcone (HymnPro) through the inhibition of tubulin polymerization. J Agri Food Chem 61:12588–12597

11. Lee JM, Lee MS, Koh D, Lee YH, Lim Y, Shin SY (2014) A new synthetic 2′-hydroxy-2,4,6-trimethoxy-5′,6′-naphthochalcone induces G2/M cell cycle arrest and apoptosis by disrupting the microtubular network of human colon cancer cells. Cancer Lett 354:348–354

12. Shin SY, Lee JM, Lee MS, Koh D, Jung H, Lim Y, Lee YH (2014) Targeting cancer cells via the reactive oxygen species-mediated unfolded protein response with a novel synthetic polyphenol conjugate. Clin Cancer Res 20:4302–4313

13. Trachootham D, Zhou Y, Zhang H, Demizu Y, Chen Z, Pelicano H, Chiao PJ, Achanta G, Arlinghaus RB, Liu J, Huang P (2006) Selective killing of oncogenicallytransformed cells through a ROS-mediated mechanism by beta-phenylethyl isothiocyanate. Cancer Cell 10:241–252

14. Raj L, Ide T, Gurkar AU, Foley M, Schenone M, Li X, Tolliday NJ, Golub TR, Carr SA, Shamji AF, Stern AM, Mandinova A, Schreiber SL, Lee SW (2011) Selective killing of cancer cells by a small molecule targeting the stress response to ROS. Nature 475:231–234

15. Silva MF, Pruccoli L, Morroni F, Sita G, Seghetti F, Viegas C, Tarozzi A (2018) The Keap1/Nrf2-ARE pathway as a pharmacological target for chalcones. Molecules 23(7):1803

16. Huang C, Monte A, Cook JM, Kabir MS, Peterson KP (2013) Zebrafish heart failure models for the evaluation of chemical probes and drugs. Assay Drug Dev Technol 11:561–572

17. Bedoukian TH (2011) Bed bug control and repellency. US Patent. US20120046359 A1

18. Hoffman RM (1991) In vitro sensitivity assays in cancer: a review, analysis, and prognosis. J Clin Lab Anal 5:133–143

19. Danial N, Korsmeyer SJ (2004) Cell death: critical control points. Cell 116:205–219

20. Zheng ZH, Dong YS, Zhang H, Lu XH, Ren X, Zhao G, He JG, Si SY (2007) Isolation and characterization of N98–1272 A, B and C, selective acetylcholinesterase inhibitors from metabolites of an actinomycete strain. J Enzyme Inhib Med Chem 22:43–49

21. Lee Y, Koh D, Lim Y (2018) 1H and 13C NMR spectral assignments of 25 ethyl 2-oxocyclohex-3-enecarboxylates. MagnReson Chem 56:1188–1200

22. Franken NAP, Rodermond HM, Stap J, Haveman J, van Bree C (2006) Clonogenic assay of cells in vitro. Nat Protoc 1:2315–2319

23. Shin SY, Lee J, Park J, Lee Y, AhnS LJH, Koh D, Lee YH, Lim Y (2019) Design, synthesis, and biological activities of 1-aryl-(3-(2-styryl)phenyl)prop-2-en-1-ones. Bioorg Med Chem 83:438–449

24. Lee YH, Park J, AhnS LY, Lee J, Shin SY, Koh D, Lim Y (2019) Design, synthesis, and biological evaluation of polyphenols with 4,6-diphenylpyrimidin-2-amine derivatives for inhibition of Aurora kinase A. Daru 27(1):265–281

25. Shin SY, Yoon H, Ahn S, Kim D, Kim SH, Koh D, Lee YH, Lim Y (2013) Chromenylchalcones showing cytotoxicity on human colon cancer cell lines and in silico docking with aurora kinases. Bioorg Med Chem 21:4250–4258

26. Gil HN, Jung E, Koh D, Lim Y, Lee YH, Shin SY (2019) A synthetic chalcone derivative, 2-hydroxy-3′,5,5′-trimethoxychalcone (DK-139), triggers reactive oxygen species-induced apoptosis independently of p53 in A549 lung cancer cells. Chem Biol Interact 298:72–79

27. Cheung J, Rudolph MJ, Burshteyn F, Cassidy MS, Gary EN, Love J, Franklin MC, Height JJ (2012) Structures of human acetylcholinesterase in complex with pharmacologically important ligands. J Med Chem 55:10282–10286

28. Kim BS, Shin SY, Ahn S, Koh D, Lee YH, Lim Y (2017) Biological evaluation of 2-pyrazolinyl-1-carbothioamide derivatives against HCT116 human colorectal cancer cell lines and elucidation on QSAR and molecular binding modes. Bioorg Med Chem 25:5423–5432

29. Lazebnik YA, Kaufmann SH, Desnoyers S, Poirier GG, Earnshaw WC (1994) Cleavage of poly(ADP-ribose) polymerase by a proteinase with properties like ICE. Nature 371:346–347

30. McHardy SF, Wang HL, McCowenSV VMC (2017) Recent advances in acetylcholinesterase Inhibitors and Reactivators: an update on the patent literature (2012–2015). Expert OpinTher Pat 27(4):455–476

31. Du A, Xie J, Guo K, Yang L, Wan Y, Yang QO, Zhang X, Niu X, Lu L, Wu J, Zhang X (2015) A novel role for synaptic acetylcholinesterase as an apoptotic deoxyribonuclease. Cell Discov 1:15002

32. Zhang XJ, Yang L, Zhao Q, Caen JP, He HY, Jin QH, Guo LH, Alemany M, Zhang LY, Shi YF (2002) Induction of acetylcholinesterase expression during apoptosis in various cell types. Cell Death Differ 9:790–800

33. Yu H, Xia H, Tang Q, Xu H, Wei G, Chen Y, Dai X, Gong Q, Bi F (2017) Acetylcholine acts through M3 muscarinic receptor to activate the EGFR signaling and promotes gastric cancer cell proliferation. Sci Rep 7:40802

34. Spinde IER (2016) Cholinergic Targets in Lung Cancer. Curr Pharm Des 22(14):2152–2159

35. Song P, Sekhon H, Proskocil B, Blusztajn JK, Mark GP, Spindel ER (2003) Synthesis of acetylcholine by lung cancer. Life Sci 72:2159–2168

36. Karpe IR, Sternfeld M, Ginzberg D, Guhl E, Graessmann A, Soreq H (1996) Overexpression of alternative human acetylcholinesterase forms modulates process extensions in cultured glioma cells. J Neurochem 66:114–123

37. Sáez-Valero J, Poza-Cisneros G, Vidal CJ (1996) Molecular forms of acetyl- and butyrylcholinesterase in human glioma. Neurosci Lett 206:173–176

38. Sáez-Valero J, Vidal CJ (1996) Biochemical properties of acetyl- and butyrylcholinesterase in human meningioma. Biochim Biophys Acta 1317:210–218

39. García-Ayllón MS, Sáez-Valero J, Piqueras-Pérez C, Vidal CJ (1999) Characterization of molecular forms of acetyl- and butyrylcholinesterase in human acoustic neurinomas. Neurosci Lett 274:56–60

40. Frucht H, Jensen RT, Dexter D, Yang WL, Xiao Y (1999) Human colon cancer cell proliferation mediated by the M3 muscarinic cholinergic receptor. Clin Cancer Res 5:2532–2539

41. Raufman J, Cheng K, Saxena N, Chahdi A, Belo A, Khurana S, Xie G (2011) Muscarinic receptor agonists stimulate matrix metalloproteinase 1-dependent invasion of human colon cancer cells. Biochem Biophys Res Commun 415:319–324

42. Belo A, Cheng K, Chahdi A, Shant J, Xie G, Khurana SJ, Raufman (2011) Muscarinic receptor agonists stimulate human colon cancer cell migration and invasion. Am J Physiol Gastrointest Liver Physiol 300(5):G749–G760

43. Cheng K, Samimi R, Xie G, Shant J, Drachenberg C, Wade M, Davis RJ, Nomikos G, Raufman JP (2008) Acetylcholine release by human colon cancer cells mediates autocrine stimulation of cell proliferation. Am J Physiol Gastrointest Liver Physiol 295:G591–G597

44. Zheng Z, Dong Y, ZhangH LuX, Ren X, Zhao G, He J, Si S (2007) Isolation and characterization of N98–1272 A, B and C, selective acetylcholinesterase inhibitors from metabolites of an actinomycete strain. J Enzyme Inhib Med Chem 22(1):43–49

45. Birks JS, Harvey RJ (2018) Donepezil for dementia due to Alzheimer's disease. Cochrane Database Syst Rev 6(6):CD001190

46. Kryger G, Harel M, Giles K, Toker L, Velan B, Lazar A, Kronman C, Barak D, Ariel N, Shafferman A, Silman I (2000) Structures of recombinant native and E202Q mutant human acetylcholinesterase complexed with the snake-venom toxin fasciculin-II. Acta Crystallogr D Biol Crystallogr 56:1385–1394

47. NachonF CE, Ronco C, Trovaslet M, Nicolet Y, Jean L, Renard P (2013) Crystal structures of human cholinesterases in complex with huprine W and tacrine: elements of specificity for anti-Alzheimer's drugs targeting acetyl- and butyryl-cholinesterase. Biochem J 453:393–399

48. Wallace AC, LaskowskiRA ThorntonJM (1995) LIGPLOT: a program to generate schematic diagrams of protein-ligand interactions. Protein Eng 8(2):127–134
49. Kuntz ID, Chen K, Sharp KA, Kollman PA (1999) The maximal affinity of ligands. Proc Natl Acad Sci USA 96(18):9997–10002
50. Boyd SM, Kloe GE (2010) Fragment library design: efficiently hunting drugs in chemical space. Drug Discov Today Technol 7(3):e147-202

Publisher's Note

Springer Nature remains neutral with regard to jurisdictional claims in published maps and institutional affiliations.